Published in final edited form as:
Circ Res. 2003 October 31; 93(9): e88–e97. doi:10.1161/01.RES.0000099243.20096.FA.

Paracrine Regulation of Angiogenesis and Adipocyte Differentiation During In Vivo Adipogenesis

Dai Fukumura[*], **Akira Ushiyama**[*], **Dan G. Duda**[*], **Lei Xu**, **Joshua Tam**, **V. Krishna K. Chatterjee**, **Igor Garkavtsev**, and **Rakesh K. Jain**
From the Edwin L. Steele Laboratory (D.F., A.U., D.G.D., L.X., J.T., I.G., R.K.J.), Department of Radiation Oncology, Massachusetts General Hospital and Harvard Medical School, Boston, Mass; Department of Medicine (K.K.C.), University of Cambridge, Cambridge, UK

Abstract

With an increasing incidence of obesity worldwide, rational strategies are needed to control adipogenesis. Growth of any tissue requires the formation of a functional and mature vasculature. To gain mechanistic insight into the link between active adipogenesis and angiogenesis, we developed a model to visualize noninvasively and in real time both angiogenesis and adipogenesis using intravital microscopy. Implanted murine preadipocytes induced vigorous angiogenesis and formed fat pads in a mouse dorsal skin-fold chamber. The newly formed vessels subsequently remodeled into a mature network consisting of arterioles, capillaries, and venules, whereas the preadipocytes differentiated into adipocytes as confirmed by increased aP2 expression. Inhibition of adipocyte differentiation by transfection of preadipocytes with a peroxisome proliferator-activated receptor γ dominant-negative construct not only abrogated fat tissue formation but also reduced angiogenesis. Surprisingly, inhibition of angiogenesis by vascular endothelial growth factor receptor-2 (VEGFR2) blocking antibody not only reduced angiogenesis and tissue growth but also inhibited preadipocyte differentiation. We found that part of this inhibition stems from the paracrine interaction between endothelial cells and preadipocytes and that VEGF–VEGFR2 signaling in endothelial cells, but not preadipocytes, mediates this process. These findings reveal a reciprocal regulation of adipogenesis and angiogenesis, and suggest that blockade of VEGF signaling can inhibit in vivo adipose tissue formation.

Keywords

obesity; adipogenesis; angiogenesis; vascular endothelial growth factor; peroxisome proliferator-activated receptor γ

Adipose tissue exhibits angiogenic activity.[1,2] recent report demonstrated that established adipose tissue mass can actually be regulated through the vasculature.[3] Importantly, the potential to acquire new fat cells from fat cell precursors throughout one's lifespan is now undisputed.[4] Thus, understanding the mechanistic relationship between adipocyte differentiation and neovascularization during de novo fat tissue formation is critical and has important implications. We used intravital microscopy[5] along with appropriate animal models

Correspondence to Rakesh K. Jain, Department of Radiation Oncology, Massachusetts General Hospital, 100 Blossom St, COX-7, Boston, MA 02114. jain@steele.mgh.harvard.edu.
Present address of A.U. is the Department of Environmental Health, National Institute of Public Health, Tokyo, Japan.
[*]These authors contributed equally to this work.

and optical probes to monitor and quantify dynamic biological events, including angiogenesis, noninvasively and in real time. To investigate the relationship between adipogenesis and angiogenesis, we adapted the in vivo fat pad formation model by implanting 3T3-F442A murine preadipocytes[4,6,7] to a mouse dorsal skin chamber[5] in severe combined immunodeficient (SCID) mice. For gene expression analyses, we implanted 3T3-F442A preadipocytes subcutaneously and recovered the fad pads at different time points. This experimental design enabled us to monitor, in parallel, both the kinetics of angiogenesis and adipogenesis and the gene expression patterns during fat tissue formation.

During the early phase of adipocyte differentiation, two families of transcriptional factors, CCAAT/enhancer binding protein (C/EBP) and peroxisome proliferator-activated receptor (PPAR) are induced.[4,8,9] Activation of PPARγ in adipogenesis is well characterized and is considered an absolute requirement for adipocyte differentiation.[10–12] To elucidate the causal link between adipocyte differentiation and angiogenesis, we introduced a dominant-negative PPARγ mutant construct into 3T3-F442A cells before implantation using an adenoviral vector, as described previously.[13] Mature, terminally differentiated adipocytes express multiple genes and proteins including aP2 (an adipocyte-specific fatty acid binding protein, originally identified as 422), FAT/CD36, perilipin, adipsin, stearoyl-CoA desaturase (SCD1), glucose transporter (GLUT4), phosphenolpyruvate carboxykinase (PEPCK), and leptin.[4,8,9] Among these, the adipocyte-specific *aP2* gene is a downstream target of PPARγ activation and is the most widely used adipocyte differentiation marker.[14,15] Thus, in this study, the kinetics of aP2 expression was used to confirm the differentiation of 3T3-F442A cells.

Angiogenesis often precedes adipose tissue formation in developing tissue, which indicates the requirement of blood vessels for tissue formation and hints at a potential direct link between angiogenesis and adipogenesis.[16] Vascular endothelial growth factor receptor 2 (VEGFR2) is expressed on vascular endothelial cells and its signaling is critical in both physiological and pathological angiogenesis.[17] Among its ligands, VEGF-A is highly expressed in adipose tissue and its expression increases significantly during adipocyte differentiation. [18–21] To assess the importance of VEGFR2 signaling in angiogenesis, vessel remodeling, and adipocyte differentiation during fat tissue formation, we determined the effect of a VEGFR2 blocking antibody[22] on angiogenesis, tissue formation, 3T3-F442A cell morphology, and changes in aP2 expression.

Materials and Methods

Cell Lines and Animals

Male SCID mice, 8 to 12 weeks old, were bred and maintained in our defined flora facility and used in all experiments. All procedures were carried out according to the Public Health Service Policy on Humane Care of Laboratory Animals and approved by the Institutional Animal Care and Use Committee. The 3T3-F442A preadipocytes (a generous gift from Dr Bruce Spiegelman, Dana-Farber Cancer Institute, Boston, Mass) and NIH 3T3 fibroblasts were maintained in Dulbecco's Minimum Essential Medium (DMEM, Gibco BRL), supplemented with 10% calf serum, glucose, L-glutamine, penicillin, and streptomycin. A murine endothelial cell line (MECs, CRL-1927) was obtained from ATCC (Manassas, Va) and cultured as recommended by the provider. For cell identification in vivo, preadipocytes were transfected by the calcium phosphate method with the green fluorescent protein (GFP) gene under the control of the *EF1α* promoter.[23] For adipogenesis inhibition, preadipocytes were transduced with a recombinant adenovirus encoding a PPARγ–dominant-negative (PPARγ-DN) mutant receptor, or mock adenovirus, as previously described.[13] Briefly, a multiplicity of infection of 10^3 for 90 minutes was used for transfection of confluent (growth arrested) preadipocytes. The efficiency of the PPARγ-DN construct was assessed functionally, ie, by evaluating the cell differentiation (online Figure, available in the online data supplement at

http://www.circresaha.org). For in vivo experiments, transfected cells were implanted 2 days after infection.

In Vivo Microscopy Using the Transparent Chamber Model

Dorsal skinfold chambers were implanted in mice, as described elsewhere.[24] Cell pellets containing 2×10^5 preadipocytes were implanted in the center of the chamber. In vivo microscopy using epi-fluorescence and multiphoton techniques was performed 1 to 2 times a week up to 4 weeks after the implantation and was followed by off-line analysis of vascular parameters as described.[24] Five random locations in the area of implantation were observed for each animal and time point. The number of nonbranching blood vessel segments (number of segments per unit area), functional vascular density (total length of perfused blood vessels per unit area), vessel diameter, and vessel volume density (calculated blood vessel volume, based on length and diameter of each segment, per unit area) were determined as described elsewhere.[24] Angiogenesis and subsequent vessel remodeling were analyzed in three different experimental settings: after implantation of NIH 3T3 or 3T3-F442A; after implantation of GFP/3T3-F442A infected with PPARγ-DN or mock adenovirus; and after implantation of GFP/3T3-F442A in mice treated with DC101 or rat IgG. In vivo observation using multiphoton laser-scanning microscopy was used as previously described.[25]

Reagents and Dosage

For VEGFR2 signaling blockade experiments, preadipocytes were implanted in dorsal skinfold chambers, and the mice were divided into two groups. In one group, rat anti-mouse VEGFR2 monoclonal antibody administration (DC101, ImClone Systems Inc, New York, NY, a generous gift from Drs D. Hicklin and P. Bohlen) was started on the day of implantation and continued every 3 days for 4 weeks. DC101 was delivered intraperitoneally at a dose of 40 mg/kg body weight, which was demonstrated previously to have blocking effects in vivo.[26–28] The control group received 40 mg/kg body weight of nonspecific isotype-matched rat IgG intraperitoneally on the same schedule.

For in vitro studies, recombinant mouse VEGF was obtained from R&D Systems and used at concentrations of 0 to 100 ng/mL. Rat IgG and DC101 were used at doses previously shown to have blocking effects in vitro.[29]

Subcutaneous Fat Pad Formation

Cell suspensions containing 1.5×10^7 cells in 100 μL of PBS were injected into the flank of SCID mice, as described.[7] For the antiadipogenesis studies, mice were divided into 3 groups with the following cell implants: GFP/3T3-F442A, GFP/3T3-F442A expressing PPARγ-DN, and GFP/3T3-F442A mock-transfected. For the antiangiogenesis experiments, GFP/3T3-F442A cells were implanted in 3 groups of mice. These mice received DC101, nonspecific IgG, or vehicle (PBS), respectively. Fat pad formation was allowed to proceed for 4 weeks, after which mice were euthanized and tissue was harvested. Tissue formed by the implanted preadipocytes was recovered using microscissors and fluorescence microscope-guided dissection. Tissue samples were snap-frozen for subsequent RNA extraction.

Histology

Tissue samples were harvested and fixed at 4 weeks after implantation. Frozen sections were used for fluorescence immunostaining using a Phyco-Erythrin anti–α-smooth muscle actin antibody (Sigma), whereas adipose cells were identified by their constitutive GFP expression. DAPI diacetate (Molecular Probes) staining of cell nuclei was used for counterstaining. Quantitation of the GFP-positive tissue area was performed in 5 nonsequential transverse sections of the fat tissue generated in the skin chambers, by calculating the area of tissue inside

the perimeter of the GFP-positive tissue (3 spots/section, n=5 mice). The area occupied by nuclei was considered a measure of the number of cells within the tissue. Images were acquired using the OpenLab software (Improvision Inc) from a fluorescence microscope (Olympus Co, Ltd, Japan, ×20 objective) equipped with a CCD camera. After processing images with Adobe Photoshop software (Adobe Systems Inc), binary images were quantified for tissue/cell area using a macro designed by Dr L.L. Munn (Massachusetts General Hospital, Boston, Mass) in the NIH Image software. Resin embedding with routine toluidine-blue counterstaining was used for morphological analyses.

Analyses of Gene Expression

Total RNA was extracted from cells and tissue samples using Triazol (Gibco BRL) following the protocol recommended by the manufacturer. Ten micrograms of total RNA were separated on an agarose gel and transferred to nylon membranes. Northern blots were probed with PCR-generated cDNA fragments. Nested primers were used to generate specific amplification products. Primers for PCR (sense, 5′-CTGGAAGACAGCTCCTCCTCGAAG-3′ and 5′-ATGTGTGATGCCTTTGTGGGAAC-3′; antisense, 5′-TAATCAACATAACCATATCCAAT-3′) were synthesized based on the mouse *aP2* gene sequence (GenBank No. NM_024406).

In Vitro Preadipocyte Differentiation Assay

To investigate the effect of VEGF on in vitro differentiation of preadipocytes, 3T3-F442A cells were grown to confluence in media supplemented with calf serum (CS, maintenance media) and exposed to increasing concentrations of murine recombinant VEGF (R&D Systems) from 0 to 100 ng/mL. In addition to VEGF, in some experiments, the culture medium was conditioned with blocking concentrations of DC101 or rat IgG both in the maintenance media (10% CS) and in the differentiation media (containing 10% FBS). To investigate the paracrine effects of VEGF, murine endothelial cells were cultured with the addition of recombinant murine VEGF and in vitro blocking concentration of DC101 (5 μg/mL). For controls, isotype-matched IgG antibody was added at similar concentrations. Twenty-four-hour–conditioned media from the endothelial cells was added to confluent cultures of preadipocytes and changed every other day. Cells were harvested at day 11 (when cell differentiation started to become apparent morphologically) to analyze the difference in aP2 expression between groups.

MTT Assay

Five hundred preadipocytes or fibroblasts were plated in 96-well plates and mouse recombinant VEGF (50 ng/mL) was added along with PBS, DC101 (1 μg/mL), or rat IgG (1 μg/mL). The MTT assay was performed at day 4, when the cells were still subconfluent in all wells. Before the assay, culture media were removed and replaced with 100 μL of fresh media and 10 μL of sterile tetrazolium salt; MTT (3[4,5-dimethylthiazol-2-yl]-2,5-diphenyl-tetrazolium bromide, Sigma) was then added to each well and incubated for 4 hours at 37°C. Finally, 100 μL of 10% SDS was added, and after incubation at 37°C overnight, the plate was read at 490 nm. The optical density values were normalized to that of the PBS-treated cells and were used as a measure of cell viability. To assess the paracrine effect of VEGF on preadipocyte proliferation, cells were plated in a similar fashion, with conditioned media from EC cultured in the presence of VEGF and blocking concentrations of DC101 or IgG. At day 4, the assay was performed as described, and the optical density value was normalized to the optical density of cells cultured in nonconditioned media.

Results

Preadipocytes Induce Angiogenesis and Vessel Remodeling In Vivo

Macroscopically, after preadipocyte implantation, the tissue reddened at the site of active angiogenesis (Figures 1A and 1B). Angiogenic vessels infiltrated the adipose cell pellet implanted on top of the host subcutaneous tissue and striated muscle layer, in which preexisting host vessels were detectable (Figures 1C and 1D; online Movie, available in the online data supplement at http://www.circresaha.org). The neovascular network induced by the preadipocyte implant was initially immature and resembled the vascular plexus during development, with relatively large vessel diameter and no morphological vessel differentiation (Figure 1E). With time, these vessels induced by the preadipocyte implant gradually reorganized (Figures 1F through 1H): mesh-like patterns of angiogenic vessels turned into a dense capillary network (Figures 1G and 1H), with arterioles and venules becoming apparent (Figure 1H). The number of blood vessel segments (Figure 2A) and vessel density (total length of blood vessels per unit tissue area; Figure 2B) increased, accompanied by a decrease in mean vessel diameter (Figure 2C) as the blood vessels remodeled. The total volume of blood vessels per unit tissue area did not change during the remodeling process (Figure 2D). The blood vessel size distribution narrowed with the remodeling of the vessel network (Figure 2E). The remodeled blood vessels were covered by α-SMA–positive cells (data not shown). The angiogenic response was specific to preadipocytes, as NIH 3T3 fibroblasts did not induce appreciable vessel formation or tissue mass (data not shown). These findings indicate that preadipocytes have the unique ability to induce in vivo angiogenesis and remodeling of vessels into efficient networks with a mature, stable architecture (characterized by small diffusion distances from vessels to parenchymal cells).

Preadipocytes Differentiate Into Mature Adipocytes In Vivo

One prominent characteristic of cell differentiation into adipocytes is the accumulation of triglyceride-containing vesicles in the cell cytosol. In tissue culture, intracellular fat droplets were observed by light microscope (Figure 3A) and were chemically stained by Oil Red O (Figure 3B). As early as after one week, some of subcutaneously implanted 3T3-442A cells acquired typical adipocyte morphology. However, the presence of host subcutaneous fat prevented the use of the Oil Red O staining in the preadipocyte implantation model. To clearly distinguish lipid accumulation in implanted cells from host-derived cells in the skinfold chamber, we induced constitutive expression of GFP in 3T3-F442A cells (hereafter referred to as GFP/3T3-F442A cells). Cytoplasmic GFP fluorescence allowed us to track implanted cells in vivo and to identify the differentiated cells, which exhibited a granular fluorescence due to lipid droplet formation (Figure 3C). Differentiation into adipocytes began several days after implantation and most of the cells acquired a mature phenotype after 4 weeks. In vivo differentiation of implanted preadipocytes was further confirmed by determining the expression levels of the adipocyte specific *aP2* gene. The expression of aP2 in the subcutaneous GFP/3T3-442A cell-derived tissue increased with time after the implantation (Figure 3D).

PPARγ-DN Inhibits Adipose Tissue Formation

To elucidate the causal link between preadipocyte differentiation and angiogenesis, we introduced a dominant-negative PPARγ mutant construct into 3T3-F442A cells before implantation using an adenoviral vector as described previously. [13] First, we confirmed the effect of PPARγ-DN on adipocyte differentiation in our model. As expected, PPARγ dominant-negative infected cells remained undifferentiated, both in vitro and in vivo (online data supplement and data not shown). In contrast to the expanding fat tissue formed by mock-transfected cells (Figure 3E), there was no tissue formation after the implantation of PPARγ dominant-negative infected cells (Figure 3F). The size of the tissue mass, the number of cells,

and the size of individual cell were significantly larger in mock-transfected cells compared with those in the PPARγ dominant-negative cells (Figures 3G and 3H).

PPARγ-DN Inhibits Angiogenesis Induced by Preadipocytes

Similar to nontransfected preadipocytes, mock-transfected preadipocytes induced extensive angiogenesis during tissue formation in vivo (Figures 4A and 4C through 4F). However, angiogenesis was significantly reduced in the PPARγ-DN cell-implanted window (Figures 4B through 4F), whereas underlying host blood vessels remained visible for the duration of the experiment (Figure 4B). Although the number of vessel segments and vessel density in mock-transfected cell implants increased with time, they remained unchanged in the PPARγ-DN cell-implanted window (Figures 4A and 4B). At later time points, mean vessel diameter was significantly larger in the PPARγ-DN group, indicating the lack of vessel remodeling (Figure 4E). Thus, the suppression of PPARγ prevented angiogenesis and subsequent vessel remodeling in vivo, rendering the preadipocytes unable to form vascularized tissue.

Anti-VEGFR2 Antibody Inhibits Angiogenesis Occurring During Adipogenesis

In agreement with the literature, VEGF-A expression was increased during in vitro differentiation of adipocytes and was highest among the various proangiogenic genes expressed by 3T3-F442A cell-derived tissue in vivo (online Table 1, available in the online data supplement at http://www.circresaha.org). To determine the relationship between VEGFR2 signaling, angiogenesis, and adipogenesis, we treated the animals with blocking concentrations of anti-VEGFR2 antibody (DC101). DC101 caused significant inhibition of both angiogenesis and subsequent vessel remodeling in GFP/3T3-F442A preadipocyte implants. In control IgG treated animals, there was robust angiogenesis and vessel maturation (Figures 5A and 5C through 5F). On the other hand, angiogenesis was significantly inhibited and underlining host blood vessels remained visible in the DC101 treated group (Figure 5B), as with the NIH3T3 or the PPAR-DN GFP/3T3-F442A cell implants. After 7 days, the DC101-treated group showed significantly fewer vessel segments and lower vessel density compared with the IgG-treated control (Figures 5C and 5D). The average vessel diameter was larger in the DC101 group (Figure 5E). Total vascular volume per unit tissue was not significantly affected (Figure 5F).

Anti-VEGFR2 Antibody Inhibits Adipose Cell Differentiation In Vivo

Implanted GFP/3T3-F442A cells showed granular GFP fluorescence indicating their differentiation into adipocytes (Figure 3C). Surprisingly, DC101 treatment not only inactivated local angiogenesis but also suppressed the differentiation of the implanted cells, which retained a fibroblast-like shape typical of undifferentiated preadipocytes (data not shown). These provocative findings were confirmed by a 6-fold reduction in aP2 expression in the tissue formed by preadipocyte implants after blockage of the VEGFR2 signaling in vivo (Figure 5G). Similarly, FAT/CD36[30,31] expression was decreased by DC101 treatment (data not shown). Collectively, these results show that VEGF-VEGFR2 signaling plays an important role in both angiogenesis and adipogenesis in preadipocyte-derived tissues.

VEGF Does Not Directly Affect Adipocyte Differentiation

To discern the mechanisms by which VEGF-VEGFR2 signaling mediates adipose tissue formation in vivo, we treated cultured 3T3-F442A cells with VEGF, anti-VEGFR2 antibody, or a combination of the two. Adipocyte differentiation was assessed by Oil Red O staining (Figure 6A). Because cell proliferation/survival was also involved in adipose tissue formation (Figure 3), we quantified cell viability by the MTT assay (Figure 6B). In vitro adipocyte differentiation and proliferation/survival were not significantly affected by exogenous VEGF or anti-VEGFR2 antibody, even at doses as high as 100 ng/mL VEGF and/or blocking doses

of DC101[29] (Figure 6). Furthermore, VEGFR2 expression, which is characteristic for endothelial cells, was undetectable in preadipocytes (online Table 1). Thus, VEGF-VEGFR2 signaling does not directly mediate adipose tissue formation derived from 3T3-F442A cells.

VEGFR2 Signaling Mediates Adipocyte Differentiation in a Paracrine Manner

To test the hypothesis that VEGFR2 signaling induces endothelial cell–derived factors that promote adipose tissue formation, we subjected confluent cultures of murine endothelial cells for 24 hours to recombinant murine VEGF and in vitro blocking concentration of DC101 or IgG. The conditioned media from endothelial cells cultured in the presence of VEGF increased preadipocyte survival/proliferation, as evinced by the MTT assay (Figure 6C), and accelerated their differentiation, revealed by an almost 3-fold increase in aP2 expression (Figure 6D). In addition, the blockade of VEGFR2 signaling reversed the effects of VEGF to a large extent. These data indicate that VEGFR2 signaling in vascular endothelial cells promotes adipogenesis in a paracrine manner and explain, in part, the mechanism by which DC101 inhibits adipogenesis in vivo.

Discussion

Our data shed new light on the complex interplay between adipose tissue formation, angiogenesis, and vessel remodeling. Angiogenesis is needed for efficient preadipocyte differentiation, but neovascularization is not triggered without adipocyte differentiation. A surprising observation involved the remodeling and maturation of angiogenic vessels. Unlike the aberrant neovascularization (driven by excess and/or unbalanced angiogenic factors) that occurs in pathological conditions such as tumors,[17] during adipose tissue formation the primary mesh-like structure matures into a normal network of new blood vessels. This is remarkable because “normal,” stable vasculature is rarely generated in currently available tissue engineering models.[32]

The molecular mechanisms underlining blood vessel maturation during de novo adipose formation are yet to be determined. Angiogenic activity of adipose tissue has been known and clinically used for treating wounds and ischemic organs for more than 400 years (documented in 1585[1,19]). Research over the last decade has uncovered pro- and antiangiogenic growth factors expressed by adipose tissues or adipocytes cultured in vitro, including VEGF-A, [18,20,33] VEGF-B,[20,33] VEGF-C,[33] Ang-1,[34] Ang-2,[35,36] PAI-1,[20,37] TGFβ,[38] leptin,[2,39] and maspin.[40] The expression and activity of these factors are interrelated. For example, leptin induces the expression of Ang-2[36] and stimulates VEGF-induced angiogenesis,[41] but represses VEGF-B expression.[42] The temporal and spatial interplay between these factors is critical for angiogenesis and subsequent vessel remodeling during adipose tissue development. Ang-2 destabilizes existing vessels and induces angiogenesis in the presence of VEGF and other angiogenic factors.[17] On the other hand, activation of the Tie2 receptor by Ang-1 mediates vessel remodeling by inducing blood vessel stabilization and maturation. The expression of angiopoietins in adipose tissue may depend on the state of cell differentiation, site of growth, and external stimuli. Further understanding of the kinetics of expression of angiogenic factors and of the corresponding morphological and functional parameters of blood vessels are warranted.

The molecular regulation of adipose differentiation has been extensively studied,[4,8,9] and PPARγ has been shown to be crucial for adipocyte differentiation.[10–12] Our approach was to use PPARγ-DN[13] to specifically inhibit the differentiation of 3T3-F442A preadipocytes before implantation. Our study confirmed that blocking the PPARγ pathway in preadipocytes inhibits not only their differentiation into adipocytes but also angiogenesis in vivo. On the other hand, PPARγ activation has pleiotropic effects, regulating different genes/functions in different cell and tissue types, including endothelial cells.[43–45] Exogenous PPARγ ligands actually inhibit

angiogenesis.[44–47] PPARγ ligands alter VEGF-A expression positively in adipocytes[21,33] and vascular smooth muscle cells,[48] whereas a decrease in VEGF-A production is induced in certain tumor cells.[45] PPARγ ligands inhibit growth and/or migration of vascular endothelial cells, smooth muscle cells, monocytes, and certain tumor cells.[43,44] Furthermore, PPARγ ligands have also been shown to reduce VEGFR1 and VEGFR2 expression on vascular endothelial cells.[46] Thus, PPARγ ligands can inhibit angiogenesis by directly affecting endothelial cells without any change in VEGF level.[47] Moreover, the VEGF promoter has not been shown to possess peroxisome proliferators response elements,[49] and by inhibiting PPAR-γ activity, we could not detect any significant change in VEGF-A expression by adipose cells (online Table 1).

A growing body of evidence shows that blood vessels are more than just carriers of nutrients and passive filters of blood in tissues. Angiogenesis precedes the development[16,50,51] and repair[52] of organs. Secreted factors from vascular endothelial cells induce proliferation and differentiation of preadipocytes,[53–55] liver organogenesis,[50] pancreas differentiation,[56] and liver protection.[57] VEGF is a critical factor in both pathological and physiological angiogenesis. Our findings show that VEGFR2 signaling in phenotypically normal, immortalized vascular endothelial cells[58] mediates the survival/proliferation and differentiation of preadipocytes, demonstrating that endothelial cells can control adipogenesis. This is in agreement with the findings reported for liver development, where VEGFR2 signaling in the endothelial cells is critical for hepatogenic cell multiplication and migration. [50] However, stimulation of mature hepatocytes is predominantly mediated through VEGFR1 signaling in liver sinusoidal endothelial cells.[57] It is conceivable that the maintenance of established adipose tissue is mediated through additional signaling pathways in the vascular endothelial cells.

Interactions between the extracellular matrix associated with angiogenic vessels and preadipocytes may also mediate adipogenesis. When Matrigel supplemented with bFGF is implanted, angiogenesis is induced followed by adipose precursor cells recruitment and fat pad formation. [59] Microvascular endothelial cells have been shown to secrete extracellular matrix components that promote preadipocyte differentiation.[55] Remodeling of extracellular matrix organization is important for both angiogenesis[17] and adipogenesis.[60] Expression of metalloproteinases such as MMP 2 and MMP 9 is increased during adipocyte differentiation[61] and both endogenous and exogenous metalloproteases induce adipogenesis. [61,62] Of particular interest, MMP-9 has been shown to increase the availability of matrix-bound VEGF in the tissue.[63] On the other hand, tissue inhibitor of metalloproteinases-3 (TIMP-3)–deficient mice exhibit increased adipose reconstitution during mammary involution.[64] Recently, TIMP-3 has been shown to inhibit angiogenesis by blocking VEGF binding to VEGFR2.[65] Inhibition of adipogenesis by TIMP-3 could be mediated by a paracrine mechanism involving endothelial VEGFR2 signaling, in agreement with our findings.

Finally, improved perfusion by newly formed vessels is required for adipocyte differentiation and tissue formation. Accordingly, the HIF-1–regulated gene *DEC1/Stra13* inhibits *PPARγ* gene expression under hypoxia.[66] Tissue oxygenation by angiogenesis and/or vessel remodeling might accelerate adipogenesis by increasing HIF-1 degradation, thereby potentiating PPARγ activation.

Taken together, our data show that the molecular and metabolic microenvironment associated with functional, mature blood vessels promotes preadipocyte differentiation and adipose tissue formation. This observation confirms that the generation of normal microcirculatory units is indispensable for organogenesis. It also raises a provocative question corresponding to the observation that most tissues have adipocytes interspersed with the organ cells: can preadipocytes be used in tissue engineering, organogenesis, and therapeutic angiogenesis? The

new adipogenesis-organogenesis model described in this study is ideal to address the mechanisms of normalization and maturation of blood vessels, and to develop and test novel strategies for tissue engineering, organogenesis, and therapeutic angiogenesis. [67] In turn, interfering with this process may provide valuable information for the identification of new targets for treating various diseases including obesity and solid tumors. Because anti-angiogenic compounds have already been demonstrated to decrease established adipose mass, [3] anti-VEGFR2 signaling agents undergoing clinical trials for cancer treatment may be useful candidates for controlling adipogenesis.

Supplementary Material

Refer to Web version on PubMed Central for supplementary material.

Acknowledgments

This study was supported by the NIH (Bioengineering Research Partnership Grant R24-CA85140). D.G. Duda is a Cancer Research Institute fellow. L. Xu is an NIH postdoctoral fellow (T32-CA73479). J. Tam is a Whitaker Foundation graduate student fellow. V.K. Chatterjee is supported by the Wellcome Trust. We thank Dr L.L. Munn for help in data analysis and thoughtful input; J. Kahn and S. Roberge for outstanding technical support; and Drs M.F. Booth, Y. Boucher, L.E. Gerweck, T.P. Padera, and B.R. Stoll for helpfulv suggestions.

References

1. Silverman KJ, Lund DP, Zetter BR, Lainey LL, Shahood JA, Freiman DG, Folkman J, Barger AC. Angiogenic activity of adipose tissue. Biochem Biophys Res Commun 1988;153:347–352. [PubMed: 2454107]
2. Sierra-Honigmann MR, Nath AK, Murakami C, Garcia-Cardena G, Papapetropoulos A, Sessa WC, Madge LA, Schechner JS, Schwabb MB, Polverini PJ, Flores-Riveros JR. Biological action of leptin as an angiogenic factor. Science 1998;281:1683–1686. [PubMed: 9733517]
3. Rupnick MA, Panigrahy D, Zhang CY, Dallabrida SM, Lowell BB, Langer R, Folkman J. Adipose tissue mass can be regulated through the vasculature. Proc Natl Acad Sci U S A 2002;99:10730–10735. [PubMed: 12149466]
4. Gregoire FM, Smas CM, Sul HS. Understanding adipocyte differentiation. Physiol Rev 1998;78:783–809. [PubMed: 9674695]
5. Jain RK, Munn LL, Fukumura D. Dissecting tumor pathophysiology using intravital microscopy. Nat Rev Cancer 2002;2:266–276. [PubMed: 12001988]
6. Green H, Kehinde O. Formation of normally differentiated subcutaneous fat pads by an established preadipose cell line. J Cell Physiol 1979;101:169–171. [PubMed: 541350]
7. Mandrup S, Loftus TM, MacDougald OA, Kuhajda FP, Lane MD. Obese gene expression at in vivo levels by fat pads derived from s.c. implanted 3T3-F442A preadipocytes. Proc Natl Acad Sci U S A 1997;94:4300–4305. [PubMed: 9113984]
8. Hwang CS, Loftus TM, Mandrup S, Lane MD. Adipocyte differentiation and leptin expression. Annu Rev Cell Dev Biol 1997;13:231–259. [PubMed: 9442874]
9. Rosen ED, Spiegelman BM. Molecular regulation of adipogenesis. Annu Rev Cell Dev Biol 2000;16:145–171. [PubMed: 11031233]
10. Rosen ED, Sarraf P, Troy AE, Bradwin G, Moore K, Milstone DS, Spiegelman BM, Mortensen RM. PPARγ is required for the differentiation of adipose tissue in vivo and in vitro. Mol Cell 1999;4:611–617. [PubMed: 10549292]
11. Ren D, Collingwood TN, Rebar EJ, Wolffe AP, Camp HS. PPARγ knockdown by engineered transcription factors: exogenous PPARγ2 but not PPARγ1 reactivates adipogenesis. Genes Dev 2002;16:27–32. [PubMed: 11782442]
12. Rosen ED, Hsu CH, Wang X, Sakai S, Freeman MW, Gonzalez FJ, Spiegelman BM. C/EBPα induces adipogenesis through PPARγ: a unified pathway. Genes Dev 2002;16:22–26. [PubMed: 11782441]
13. Gurnell M, Wentworth JM, Agostini M, Adams M, Collingwood TN, Provenzano C, Browne PO, Rajanayagam O, Burris TP, Schwabe JW, Lazar MA, Chatterjee VK. A dominant-negative

peroxisome proliferator-activated receptor gamma (PPARγ) mutant is a constitutive repressor and inhibits PPARγ-mediated adipogenesis. J Biol Chem 2000;275:5754–5759. [PubMed: 10681562]

14. Bernlohr DA, Doering TL, Kelly TJ Jr, Lane MD. Tissue specific expression of p422 protein, a putative lipid carrier, in mouse adipocytes. Biochem Biophys Res Commun 1985;132:850–855. [PubMed: 2415129]
15. Spiegelman BM, Frank M, Green H. Molecular cloning of mRNA from 3T3 adipocytes: regulation of mRNA content for glycerophosphate dehydrogenase and other differentiation-dependent proteins during adipocyte development. J Biol Chem 1983;258:10083–10089. [PubMed: 6411703]
16. Crandall DL, Hausman GJ, Kral JG. A review of the microcirculation of adipose tissue: anatomic, metabolic, and angiogenic perspectives. Microcirculation 1997;4:211–232. [PubMed: 9219215]
17. Carmeliet P, Jain RK. Angiogenesis in cancer and other diseases: from genes to function to therapy. Nature 2000;407:249–257. [PubMed: 11001068]
18. Claffey KP, Wikison WO, Spiegelman BM. Vascular endothelial growth factor: regulation by cell differentiation and activated second messenger pathways. J Biol Chem 1992;267:16317–16322. [PubMed: 1644816]
19. Zhang QX, Magovern CJ, Mack CA, Budenbender KT, Ko W, Rosengart TK. Vascular endothelial growth factor is the major angiogenic factor in omentum: mechanism of the omentum-mediated angiogenesis. J Surg Res 1997;67:147–154. [PubMed: 9073561]
20. Soukas A, Socci ND, Saatkamp BD, Novelli S, Friedman JM. Distinct transcriptional profiles of adipogenesis in vivo and in vitro. J Biol Chem 2001;276:34167–34174. [PubMed: 11445576]
21. Emoto M, Anno T, Sato Y, Tanabe K, Okuya S, Tanizawa Y, Matsutani A, Oka Y. Troglitazone treatment increases plasma vascular endothelial growth factor in diabetic patients and its mRNA in 3T3-L1 adipocytes. Diabetes 2001;50:1166–1170. [PubMed: 11334422]
22. Witte L, Hicklin DJ, Zhu Z, Pytowski B, Kotanides H, Rockwell P, Bohlen P. Monoclonal antibodies targeting the VEGF receptor-2 (Flk/KDR) as an anti-angiogenic therapeutic strategy. Cancer Metastasis Rev 1998;17:155–161. [PubMed: 9770111]
23. Chang YS, diTomasso E, McDonald DM, Jones R, Jain RK, Munn LL. Mosaic blood vessels in tumors: frequency of cancer cells in contact with flowing blood. Proc Natl Acad Sci U S A 2000;97:14608–14613. [PubMed: 11121063]
24. Leunig M, Yuan F, Menger MD, Boucher Y, Goetz AE, Messmer K, Jain RK. Angiogenesis, microvascular architecture, microhemodynamics, and interstitial fluid pressure during early growth of human adenocarcinoma LS174T in SCID mice. Cancer Res 1992;52:6553–6560. [PubMed: 1384965]
25. Brown EB, Campbell RB, Tsuzuki Y, Xu L, Carmeliet P, Fukumura D, Jain RK. In vivo measurement of gene expression, angiogenesis, and physiological function in tumors using multiphoton laser scanning microscopy. Nat Med 2001;7:864–868. [PubMed: 11433354]
26. Prewett M, Huber J, Li Y, Santiago A, O'Connor W, King K, Overholser J, Hooper A, Pytowski B, Witte L, Bohlen P, Hicklin DJ. Antivascular endothelial growth factor receptor (fetal liver kinase 1) monoclonal antibody inhibits tumor angiogenesis and growth of several mouse and human tumors. Cancer Res 1999;59:5209–5218. [PubMed: 10537299]
27. Kozin SV, Boucher Y, Hicklin DJ, Bohlen P, Jain RK, Suit HD. Vascular endothelial growth factor receptor-2-blocking antibody potentiates radiation-induced long-term control of human tumor xenografts. Cancer Res 2001;61:39–44. [PubMed: 11196192]
28. Izumi Y, Tomaso Ed, Hooper A, Huang P, Huber J, Hicklin DJ, Fukumura D, Jain RK, Suit HD. Responses to anti-angiogenesis treatment of spontaneous autochthonous tumors and their isografts. Cancer Res 2003;63:747–751. [PubMed: 12591719]
29. Rockwell P, Neufeld G, Glassman A, Caron D, Goldstein N. In vitro neutralization of vascular endothelial growth factor activation by a monoclonal antibody. Mol Cell Differ 1994;3:91–109.
30. Teboul L, Febbraio M, Gaillard D, Amri EZ, Silverstein R, Grimaldi PA. Structural and functional characterization of the mouse fatty acid translocase promoter: activation during adipose differentiation. Biochem J 2001;360:305–312. [PubMed: 11716758]
31. Sato O, Kuriki C, Fukui Y, Motojima K. Dual promoter structure of mouse and human fatty acid translocase/CD36 genes and unique transcriptional activation by peroxisome proliferator-activated receptor α and γ ligands. J Biol Chem 2002;277:15703–15711. [PubMed: 11867619]

32. Griffith LG, Naughton G. Tissue engineering: current challenges and expanding opportunities. Science 2002;295:1009–1014. [PubMed: 11834815]
33. Asano A, Irie Y, Saito M. Isoform-specific regulation of vascular endothelial growth factor (VEGF) family mRNA expression in cultured mouse brown adipocytes. Mol Cell Endocrinol 2001;174:71–76. [PubMed: 11306173]
34. Stacker SA, Runting AS, Caesar C, Vitali A, Lackmann M, Chang J, Ward L, Wilks AF. The 3T3-L1 fibroblast to adipocyte conversion is accompanied by increased expression of angiopoietin-1, a ligand for tie2. Growth Factors 2000;18:177–191. [PubMed: 11334054]
35. Guo X, Liao K. Analysis of gene expression profile during 3T3-L1 preadipocyte differentiation. Gene 2000;251:45–53. [PubMed: 10863095]
36. Cohen B, Barkan D, Levy Y, Goldberg I, Fridman E, Kopolovic J, Rubinstein M. Leptin induces angiopoietin-2 expression in adipose tissues. J Biol Chem 2001;276:7697–7700. [PubMed: 11152449]
37. Samad F, Yamamoto K, Loskutoff DJ. Distribution and regulation of plasminogen activator inhibitor-1 in murine adipose tissue in vivo: induction by tumor necrosis factor-α and lipopolysaccharide. J Clin Invest 1996;97:37–46. [PubMed: 8550848]
38. Samad F, Yamamoto K, Pandey M, Loskutoff DJ. Elevated expression of transforming growth factor-β in adipose tissue from obese mice. Mol Med 1997;3:37–48. [PubMed: 9132278]
39. Bouloumie A, Drexler HC, Lafontan M, Busse R. Leptin, the product of Ob gene, promotes angiogenesis. Circ Res 1998;83:1059–1066. [PubMed: 9815153]
40. Zhang M, Volpert O, Shi YH, Bouck N. Maspin is an angiogenesis inhibitor. Nat Med 2000;6:196–199. [PubMed: 10655109]
41. Cao R, Brakenhielm E, Wahlestedt C, Thyberg J, Cao Y. Leptin induces vascular permeability and synergistically stimulates angiogenesis with FGF-2 and VEGF. Proc Natl Acad Sci U S A 2001;98:6390–6395. [PubMed: 11344271]
42. Soukas A, Cohen P, Socci ND, Friedman JM. Leptin-specific patterns of gene expression in white adipose tissue. Genes Dev 2000;14:963–980. [PubMed: 10783168]
43. Willson TM, Lambert MH, Kliewer SA. Peroxisome proliferator-activated receptor γ and metabolic disease. Annu Rev Biochem 2001;70:341–367. [PubMed: 11395411]
44. Hsueh WA, Law RE. PPARγ and atherosclerosis: effects on cell growth and movement. Arterioscler Thromb Vasc Biol 2001;21:1891–1895. [PubMed: 11742860]
45. Panigrahy D, Singer S, Shen LQ, Butterfield CE, Freedman DA, Chen EJ, Moses MA, Kilroy S, Duensing S, Fletcher C, Fletcher JA, Hlatky L, Hahnfeldt P, Folkman J, Kaipainen A. PPARγ ligands inhibit primary tumor growth and metastasis by inhibiting angiogenesis. J Clin Invest 2002;110:923–932. [PubMed: 12370270]
46. Xin X, Yang S, Kowalski J, Gerritsen ME. Peroxisome proliferator-activated receptor γ ligands are potent inhibitors of angiogenesis in vitro and in vivo. J Biol Chem 1999;274:9116–9121. [PubMed: 10085162]
47. Murata T, Hata Y, Ishibashi T, Kim S, Hsueh WA, Law RE, Hinton DR. Response of experimental retinal neovascularization to thiazolidinediones. Arch Ophthalmol 2001;119:709–717. [PubMed: 11346398]
48. Yamakawa K, Hosoi M, Koyama H, Tanaka S, Fukumoto S, Morii H, Nishizawa Y. Peroxisome proliferator-activated receptor-γ agonists increase vascular endothelial growth factor expression in human vascular smooth muscle cells. Biochem Biophys Res Commun 2000;271:571–574. [PubMed: 10814503]
49. Fauconnet S, Lascombe I, Chabannes E, Adessi G-L, Desvergne B, Wahli W, Bittard H. Differential regulation of vascular endothelial growth factor expression by peroxisome proliferator-activated receptors in bladder cancer cells. J Biol Chem 2002;277:23534–23543. [PubMed: 11980898]
50. Matsumoto K, Yoshitomi H, Rossant J, Zaret KS. Liver organogenesis promoted by endothelial cells prior to vascular function. Science 2001;294:559–563. [PubMed: 11577199]
51. Cleaver O, Melton DA. Endothelial signaling during development. Nat Med 2003;9:661–668. [PubMed: 12778164]

52. Franck-Lissbrant I, Haggstrom S, Damber J-E, Bergh A. Testosterone stimulates angiogenesis and vascular regrowth in the ventral prostate in castrated adult rats. Endocrinology 1998;139:451–456. [PubMed: 9449610]
53. Aoki S, Toda S, Sakemi T, Sugihara H. Coculture of endothelial cells and mature adipocytes actively promotes immature preadipocyte development in vitro. Cell Struct Funct 2003;28:55–60. [PubMed: 12655151]
54. Hutley LJ, Herington AC, Shurerty W, Cheung C, Vesey DA, Cameron DP, Prins JB. Human adipose tissue endothelial cells promote preadi-pocyte proliferation. Am J Physiol Endocrinol Metab 2001;281:E1037–E1044. [PubMed: 11595661]
55. Varzaneh FE, Shillabeer G, Wong KL, Lau DCW. Extracellular matrix components secreted by microvascular endothelial cells stimulate preadipocyte differentiation in vitro. Metabolism 1994;43:906–912. [PubMed: 8028517]
56. Lammert E, Cleaver O, Melton D. Induction of pancreatic differentiation by signals from blood vessels. Science 2001;294:564–567. [PubMed: 11577200]
57. LeCouter J, Moritz DR, Li B, Phillips GL, Liang XH, Gerber H-P, Hillan KJ, Ferrara N. Angiogenesis-independent endothelial protection of liver: role of VEGFR-1. Science 2003;299:890–893. [PubMed: 12574630]
58. MacKay K, Striker LJ, Elliot S, Pinkert CA, Brinster RL, Striker GE. Glomerular epithelial, mesangial, and endothelial cell lines from transgenic mice. Kidney Int 1988;33:677–684. [PubMed: 2835539]
59. Kawaguchi N, Toriyama K, Nicodemou-Lena E, Inou K, Torii S, Kitagawa Y. De novo adipogenesis in mice at the site of injection of basement membrane and basic fibroblast growth factor. Proc Natl Acad Sci U S A 1998;95:1062–1066. [PubMed: 9448285]
60. Lilla J, Stickens D, Werb Z. Metalloproteases and adipogenesis: a weighty subject. Am J Pathol 2002;160:1551–1554. [PubMed: 12000705]
61. Bouloumie A, Marumo T, Lafontan M, Busse R. Adipocytes produces matrix metalloproteinases 2 and 9: involvement in adipose differentiation. Diabetes 2001;50:2080–2086. [PubMed: 11522674]
62. Kawaguchi N, Xiufeng X, Tajima R, Kronqvist P, Sunberg C, Loechel F, Albrechtsen R, Wewer UM. ADAM 12 protease induces adipogenesis in transgenic mice. Am J Pathol 2002;160:1895–1903. [PubMed: 12000741]
63. Bergers G, Brekken R, McMahon G, Vu TH, Itoh T, Tamaki K, Tanzawa K, Thorpe P, Itohara S, Werb Z, Hanahan D. Matrix metalloproteinase-9 triggers the angiogenic switch during carcinogenesis. Nat Cell Biol 2000;2:737–744. [PubMed: 11025665]
64. Fata JE, Leco KJ, Voura EB, Yu HE, Waterhouse P, Murphy G, Moorehead RA, Khokha R. Accelerated apoptosis in the Timp-3-deficient mammary gland. J Clin Invest 2001;108:831–841. [PubMed: 11560952]
65. Qi JH, Ebrahem Q, Moore N, Murphy G, Claesson-Welsh L, Bond M, Baker A, Anand-Apte B. A novel function for tissue inhibitor of metalloproteinases-3 (TIMP3): inhibition of angiogenesis by blockage of VEGF binding to VEGF receptor-2. Nat Med 2003;9:407–415. [PubMed: 12652295]
66. Yun Z, Maecker HL, Johnson RS, Giaccia AJ. Inhibition of PPARγ2 gene expression by the HIF-1-regulated gene *DEC1/Stra13*: a mechanism for regulation of adipogenesis by hypoxia. Dev Cell 2002;2:331–341. [PubMed: 11879638]
67. Jain RK. Molecular regulation of vessel maturation. Nat Med 2003;9:685–693. [PubMed: 12778167]

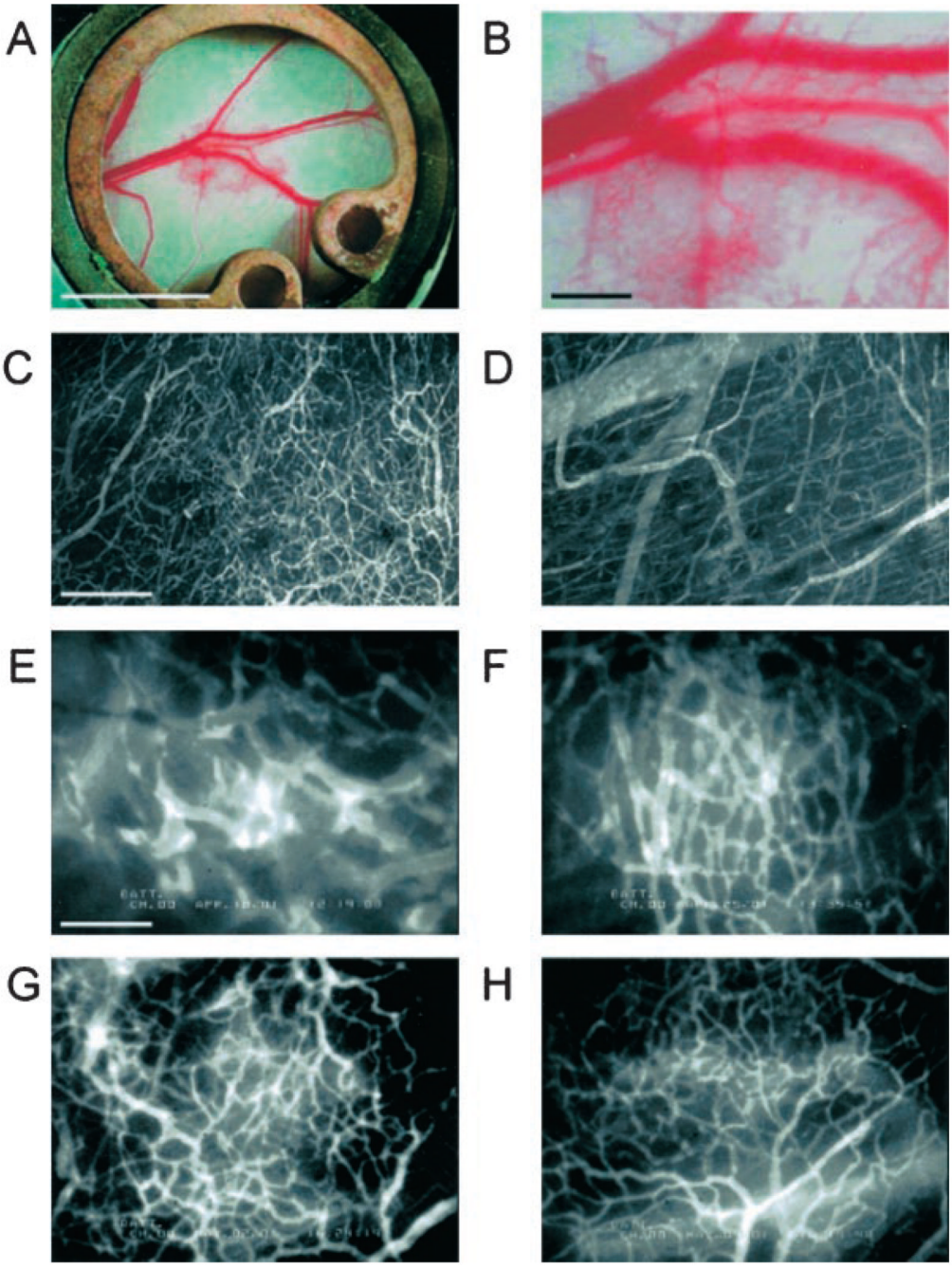

Figure 1.

Angiogenesis and vessel remodeling during adipogenesis in the mouse dorsal skinfold chamber after 3T3-F442A cell implantation. A and B, Macroscopic images 9 days after implantation. C and D, Multiphoton laser-scanning microscopy images 28 days after preadipocyte implantation. Images were obtained by maximum intensity projection of 31 optical slices, each 5 μm thick: the top 150-μm de novo adipose tissue layer (C) and the bottom 150-μm host subcutaneous layer (D). E through H, High-power microscopic images of fluorescence contrast-enhanced blood vessels at 7 days (E), 14 days (F), 21 days (G), and 28 days (H) after implantation. Bars indicate 5 mm (A), 0.5 mm (B), 200 μm (C and D), and 100 μm (E through H), respectively.

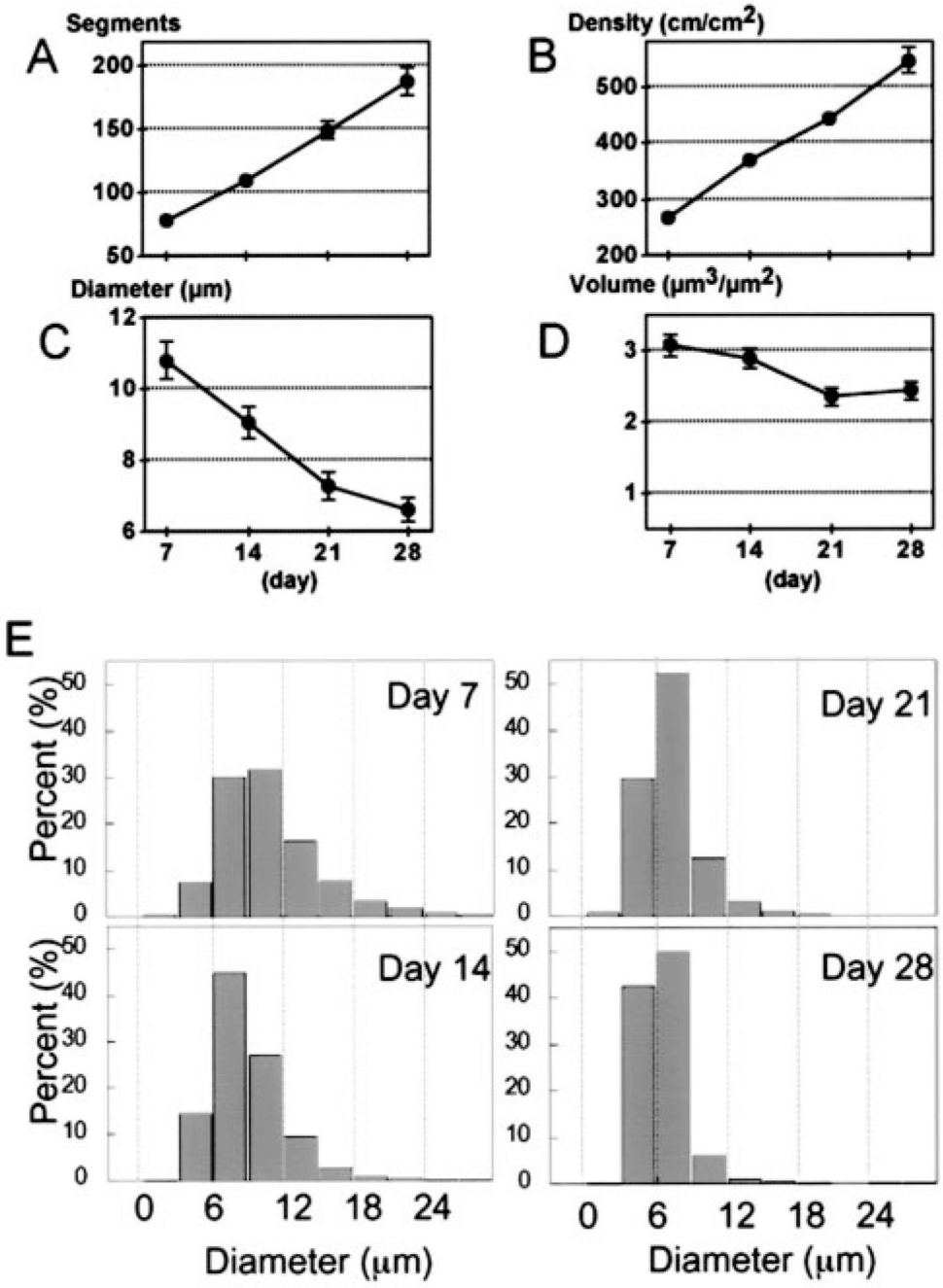

Figure 2.

Quantitative analysis of blood vessels during adipogenesis (n=7 mice). A, Number of vessel segments in the high-power view field. B, Vascular length density. C, Vessel diameter. D, Calculated blood vessel volume. E, Vessel diameter histogram. Each vessel segment was categorized by diameter and shown as a cumulative frequency distribution. Segment diameters were distributed over a wide range at day 7. Distribution shifted leftward and the range became narrow as a result of vessel remodeling with continued adipogenesis. At day 28, most segments (92%) were 3 to 9 μm in diameter.

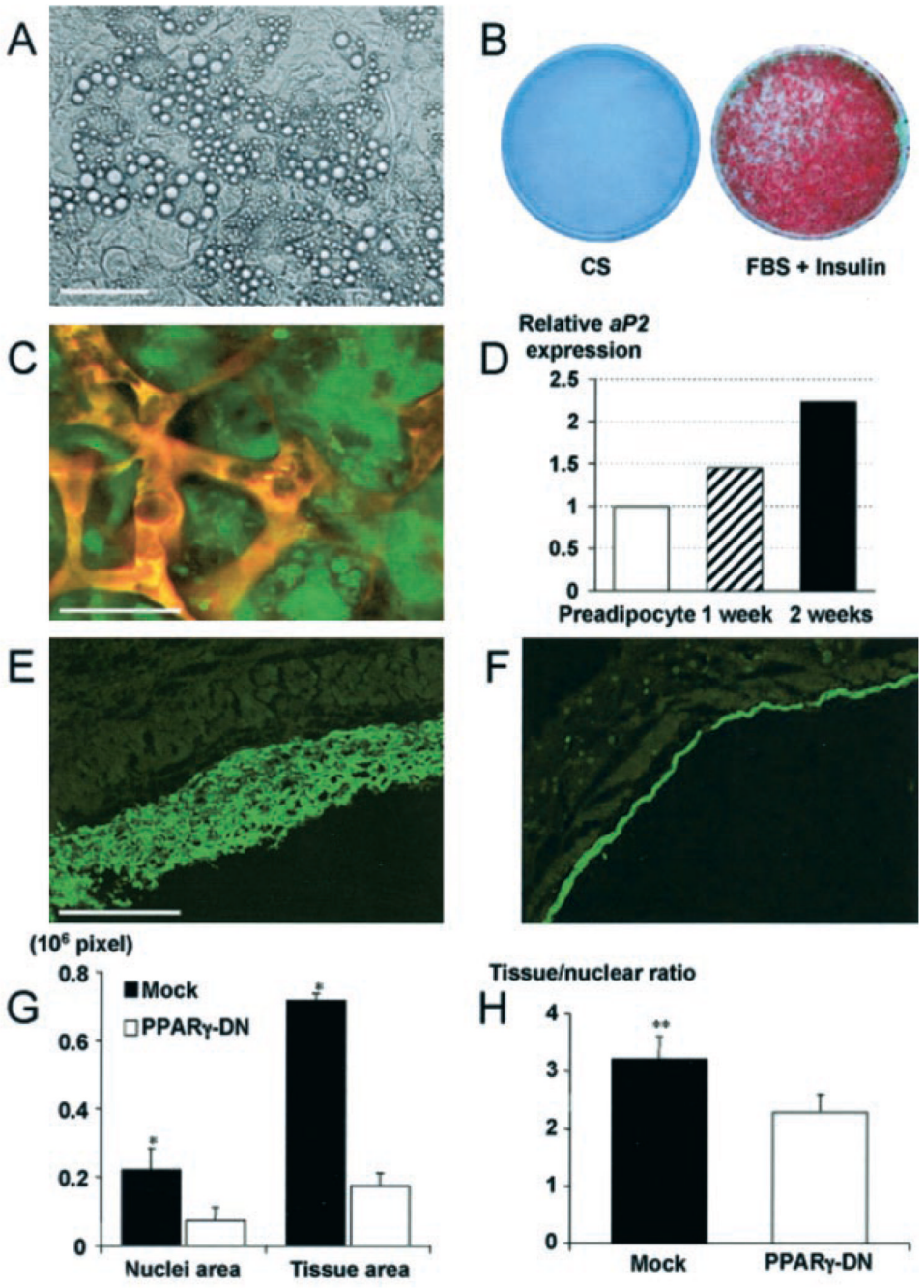

Figure 3.

Differentiation of 3T3-F442A preadipocytes and de novo adipose tissue formation: the effect of PPARγ-DN. A, Bright-field microscopic image of differentiated adipocytes in vitro. B, Macroscopic images of Oil Red O staining. C, Fluorescence image of differentiated adipocytes in vivo. To identify implanted cells in vivo, we used GFP-labeled preadipocytes. We found fat accumulation in GFP-positive cells during conversion of fibroblast-shaped preadipocytes to round-shaped adipocytes. This was visible as granular fluorescence due to fat droplets in the cytosol and was observed by multiphoton microscope (with rhodamine-dextran vessel enhancement). D, Active adipogenesis on a subcutaneous cell implant, confirmed by increasing *aP2* levels (values shown after quantitative densitometry of a Northern blot analysis). E and

F, Fluorescence microscopy in tissue sections from (E) mock- and (F) PPARγ-DN–transfected preadipocyte-generated tissues. G and H, Histological analyses of tissue expansion and cell size. G, An increased number of cells and tissue area is seen in mock preadipocyte tissue compared with PPARγ-DN tissue. H, Number of cells per tissue area is decreased in mock preadipocyte–generated tissue, documenting the increase in size of the cells in these tissues. *P<0.01 as compared with corresponding control by two-tailed t test; **P<0.05 using the Wilcoxon rank-sum test. Bars=50 μm (A), 50 μm (C), and 0.5 mm (E and F), respectively.

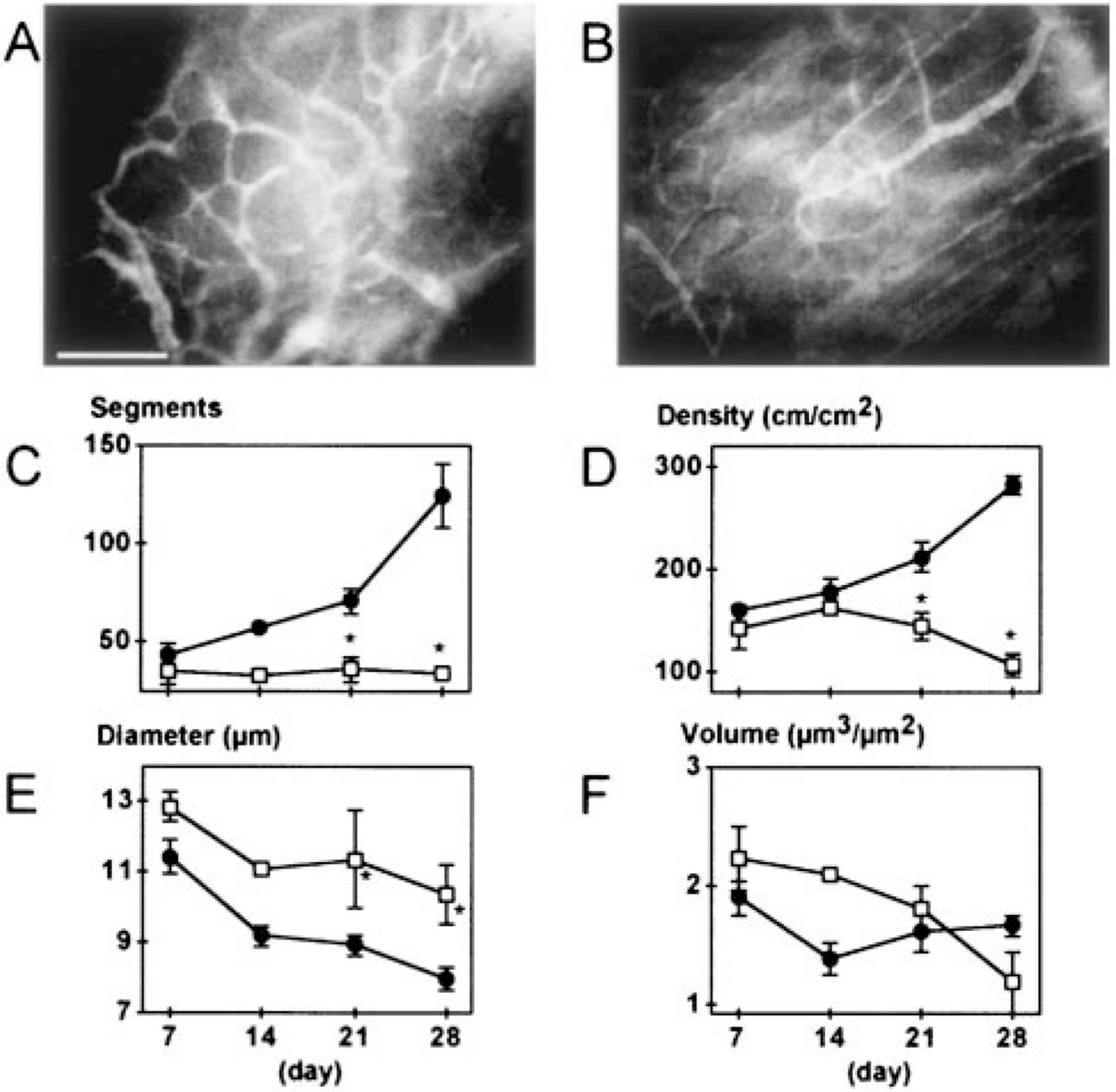

Figure 4.

Effect of PPARγ-DN on angiogenesis in the adipose tissue generated from preadipocytes. A and B, Fluorescence images of blood vessels 21 days after mock- (A) and PPARγ-DN–transfected (B) preadipocyte implantation. Bar=100 μm. C through F, Quantitative analyses of tissue neovascularization: C, number of vessel segments; D, vascular length density; E, vessel diameter; F, vessel volume. Filled circles, control (n=6); open squares, PPARγ-dominant-negative–transfected preadipocytes (n=5). There was no difference between the two different sets of control cells (mock-transfected preadipocytes, n=3 mice, and EF1α-GFP 3T3-F442A cells, n=3). These two groups are combined for presentation and statistical analysis. **P*<0.01 as compared with corresponding control by two-tailed *t* test.

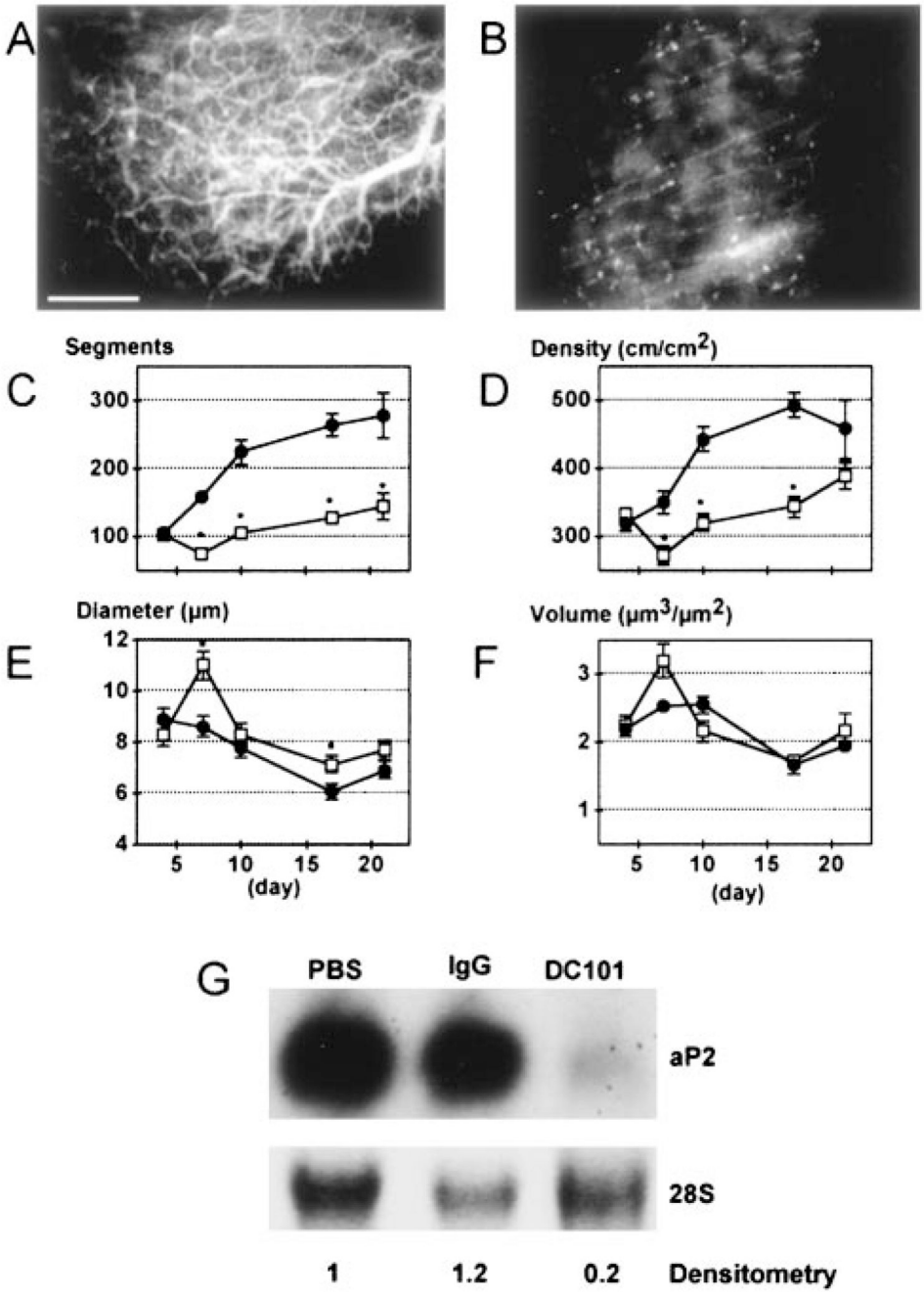

Figure 5.

Effect of VEGFR2 blockade on angiogenesis and adipogenesis. A and B, Visualization of rhodamine-dextran contrast-enhanced blood vessels 21 days after preadipocyte implantation with control IgG (A) and DC101 (B) treatments. C through F, Quantitative analyses of tissue neovascularization: C, number of vessel segments; D, vascular length density; E, vessel diameter; F, vessel volume. Filled circles represent IgG treatment (n=6 mice); open squares, DC101 treatment (n=6 mice). **P*<0.01 as compared with IgG by two-tailed *t* test. G, In vivo gene expression of aP2 in preadipocyte-generated tissue with densitometry normalized to control condition (PBS).

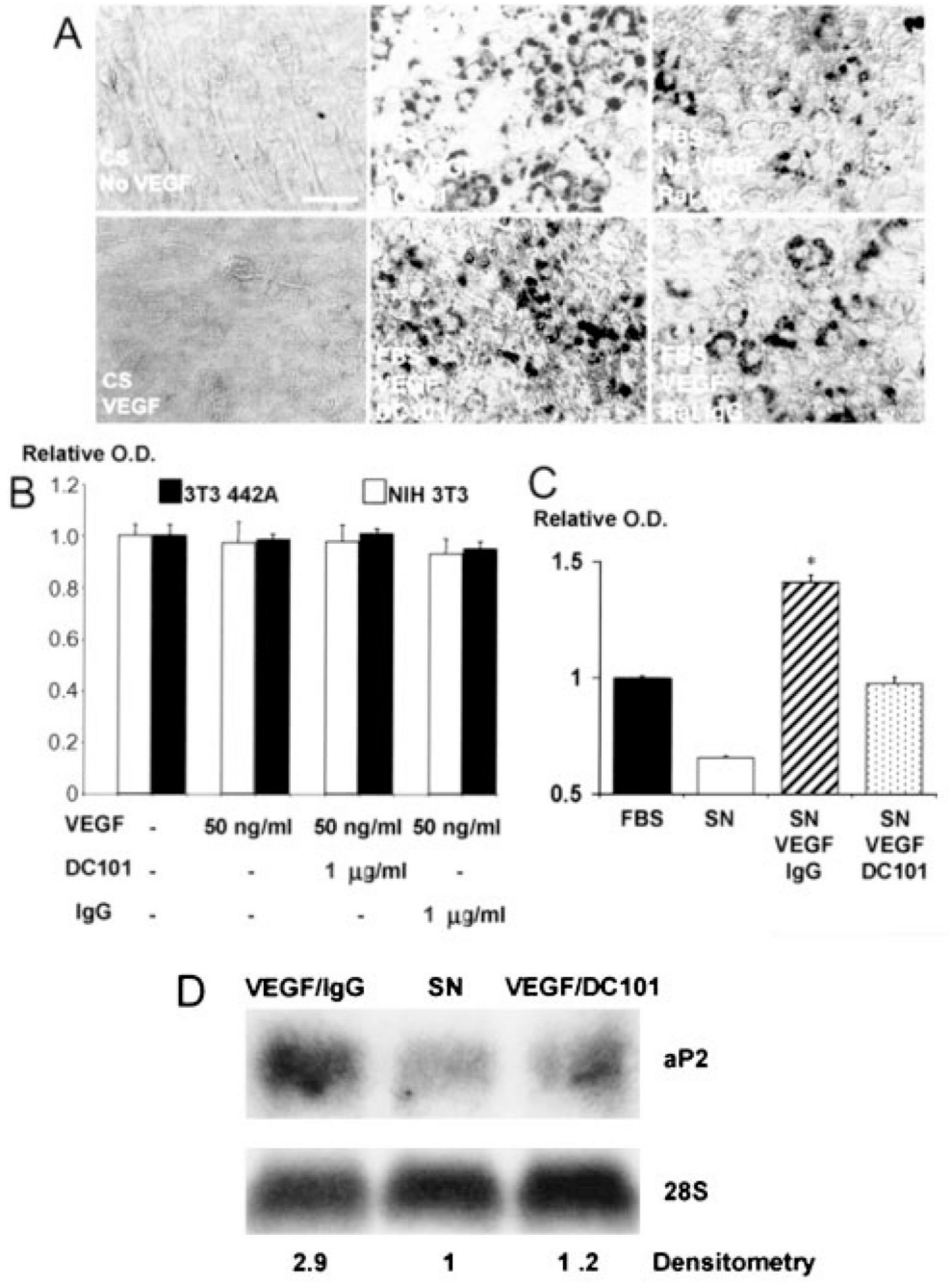

Figure 6.

Role of VEGFR2 signaling in preadipocyte differentiation and proliferation. A, Confluent 3T3-F442A cells were maintained for 11 days with either 10% calf serum (CS, maintenance media) with or without VEGF (50 ng/mL) or 10% FBS (differentiation media) and either DC101 or rat IgG (1 µg/mL). At day 11, cells were stained with Oil Red O. Mouse recombinant VEGF did not induce differentiation in preadipocytes cultured in 10% CS (maintenance media) and did not increase the differentiation rate in cells treated with 10% FBS (differentiation media). Addition of DC101 or IgG to the culture media had no effect on in vitro adipogenesis. Bar=50 µm. B, Mouse recombinant VEGF (50 ng/mL) and PBS, DC101, or rat IgG was added (concentration of the antibodies, 1 µg/mL), and the MTT assay was performed at day 4. The

optical density values were normalized to that of the PBS-treated cells and were used as a measure of viability. C, MTT assay for preadipocytes after 4 days of culture with endothelial conditioned media [FBS indicates nonconditioned culture media with 10% FBS; SN, supernatant, endothelial conditioned media cultured with 10% FBS but no other additives; SN/VEGF/IgG, endothelial conditioned media cultured with 10% FBS, VEGF (50 ng/mL) and nonspecific IgG (5 μg/mL); SN/VEGF/DC101, endothelial conditioned media cultured with 10% FBS, VEGF (50 ng/mL) and DC101 (5 μg/mL)]. Data were normalized to the control condition (FBS). *$P<0.01$ as compared with SN/VEGF/DC101 by two-tailed *t* test. Error bars represent standard error. D, In vitro gene expression of aP2 in preadipocytes after 11 days of culture with endothelial conditioned media (VEGF/IgG, endothelial conditioned media cultured with 10% FBS, VEGF, and nonspecific IgG; SN, endothelial conditioned media with 10% FBS and no other additives; VEGF/DC101, endothelial conditioned media cultured with 10% FBS, VEGF, and DC101). Fold increase in aP2 expression by differentiating preadipocytes was calculated by densitometry and normalized to the control condition (SN).